Supplementary Table and Figures

Table S1. List of the 990 genes that represent YAP-dependent, β-catenin-independent targets downstream of APC.

The Excel file also shows the relative fold change of expression in the *β-catenin*$^{\Delta ex3}$*;Sav1* double mutant jejunum or the *APC* mutant jejunum relative to the *β-catenin*$^{\Delta ex3}$ jejunum.

Figure S1. Histogram showing the proportion of human tumors with nuclear accumulation of YAP or β-catenin.

Tissue microarrays containing tubular adenomas of the colon, pancreatic acinar cell carcinomas, ovarian serous carcinomas and pancreatic ductal adenocarcinomas were examined stained for YAP and β-catenin. The percentage of tumors with and without nuclear accumulation of each protein is indicated by black and white color, respectively.

Figure S1

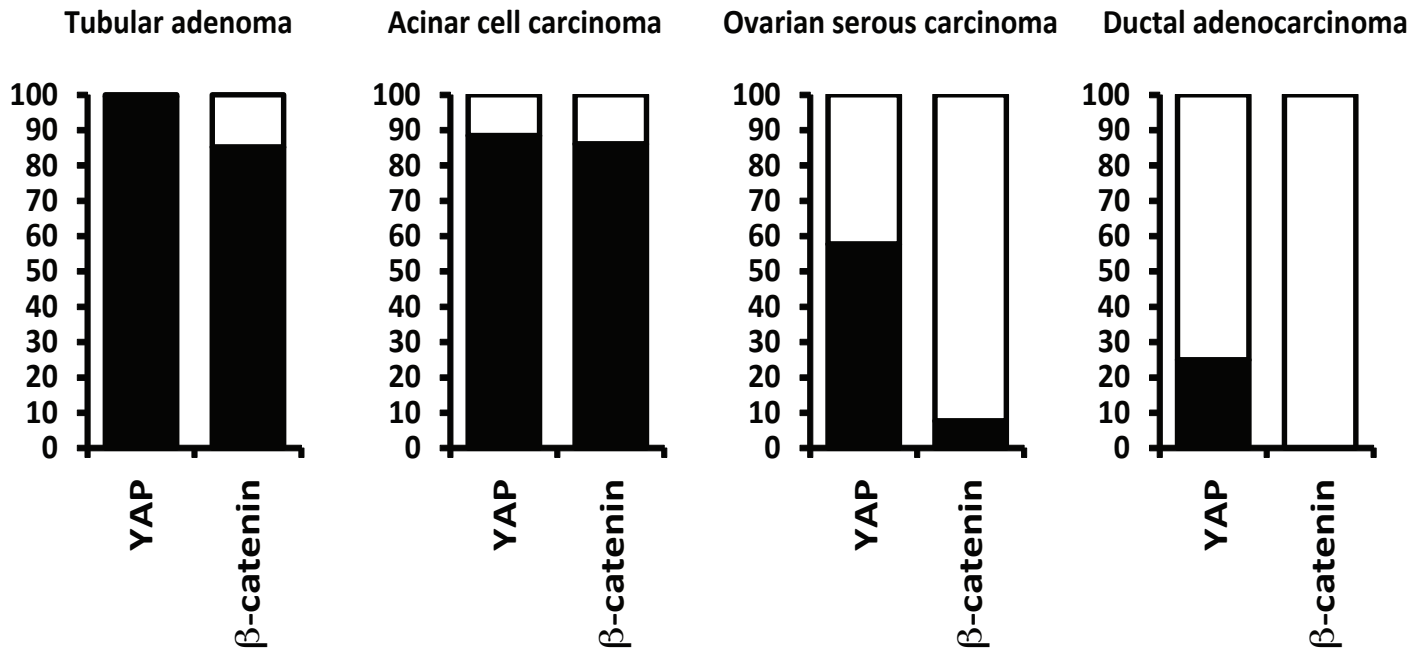
Tubular adenoma
Acinar cell carcinoma
Ovarian serous carcinoma
Ductal adenocarcinoma
100
90
80
70
60
50
40
30
20
10
0
YAP
β-catenin

Figure S2. Immunohistochemistry analysis of Lats1 in 1-month-old wild type mouse jejunum showing that Lats1 is mainly expressed in the crypt (black arrow).

Figure S2

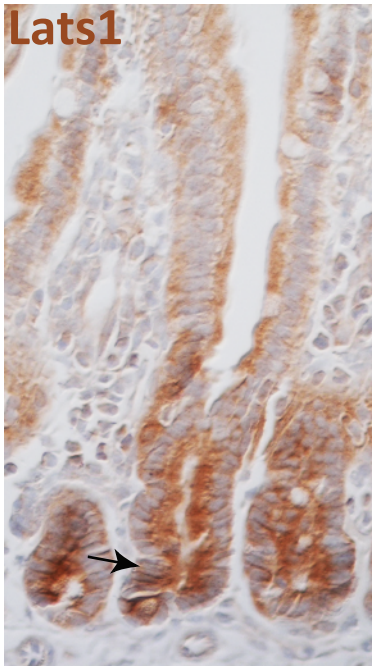

Figure S3. Further characterization of the effects of APC, rhWnt3a and GSK-3β inhibitor on the Hippo-YAP pathway.

(A-C) Co-IP analysis in HEK293 cells. Note the absence of interactions between APC and Mst2, Mob1 or YAP.

(D-E) APC overexpression did not affect Mst2-Sav1 or Lats1-Mob1 interactions.

(F) rhWnt3a did not affect Lats or YAP phosphorylation. HEK293 Cells were treated with 100 ng/ml rhWnt3a for indicated time.

(G) The tankyrase inhibitor XAV939 did not affect Lats or YAP phosphorylation. HEK293 Cells were treated with 10 μm XAV939 for indicated time.

(H-I) Co-IP analysis in HEK293 cells. BIO treatment for 1 hr did not affect Mst2-Sav1 or Lats1-Mob1 interactions.

Figure S3

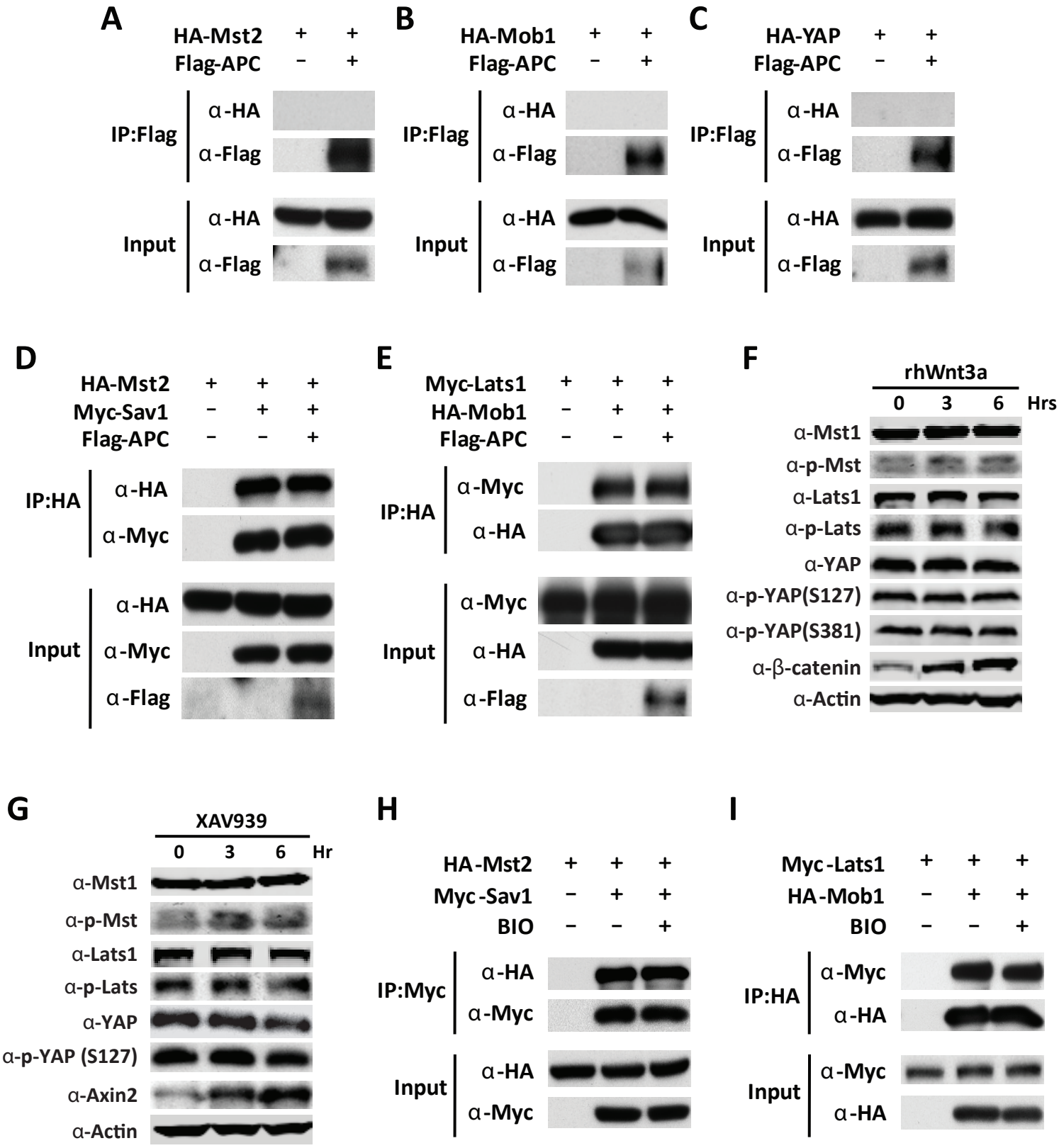
A
HA-Mst2 + +
Flag-APC − +
IP:Flag
α-HA
α-Flag
Input
α-HA
α-Flag
B
HA-Mob1 + +
Flag-APC − +
IP:Flag
α-HA
α-Flag
Input
α-HA
α-Flag
C
HA-YAP + +
Flag-APC − +
IP:Flag
α-HA
α-Flag
Input
α-HA
α-Flag
D
HA-Mst2 + + +
Myc-Sav1 − + +
Flag-APC − − +
IP:HA
α-HA
α-Myc
Input
α-HA
α-Myc
α-Flag
E
Myc-Lats1 + + +
HA-Mob1 − + +
Flag-APC − − +
IP:HA
α-Myc
α-HA
Input
α-Myc
α-HA
α-Flag
F
rhWnt3a
0 3 6 Hrs
α-Mst1
α-p-Mst
α-Lats1
α-p-Lats
α-YAP
α-p-YAP(S127)
α-p-YAP(S381)
α-β-catenin
α-Actin
G
XAV939
0 3 6 Hr
α-Mst1
α-p-Mst
α-Lats1
α-p-Lats
α-YAP
α-p-YAP (S127)
α-Axin2
α-Actin
H
HA-Mst2 + + +
Myc-Sav1 − + +
BIO − − +
IP:Myc
α-HA
α-Myc
Input
α-HA
α-Myc
I
Myc-Lats1 + + +
HA-Mob1 − + +
BIO − − +
IP:HA
α-Myc
α-HA
Input
α-Myc
α-HA

Figure S4. YAP/TAZ and β-catenin are not co-regulated by a common destruction complex through canonical Wnt signaling.

(A) rhWnt3a induced β-catenin activity (TOP-FLASH reporter), but not YAP activity (8xGTIIC-Lux reporter). HEK293 Cells were treated with 100 or 250 ng/ml rhWnt3a for indicated hours.

(B) Specificity of the luciferase reporters. The TOP-FLASH and 8xGTIIC-Lux reporters were transfected together with an activated β-catenin (S33Y, Kolligs et al., 1999) or YAP/TEAD2 into HEK293 cells. The TOP-FLASH reporter was only activated by β-catenin. Conversely, 8xGTIIC-Lux was only activated by YAP/TEAD2.

(C) rhWnt3a did not promote YAP nuclear localization. HEK293 were treated with 100 ng/ml rhWnt3a for 8 hours.

(D) β-catenin protein levels were increased after 100 or 250 ng/ml rhWnt3a treatment for 8 hours.

(E) β-catenin and YAP/TAZ staining in serial sections of *β-catenin*-deficient (*VilCre;Catnb*$^{flox/flox}$) distal colon at 1-month of age. Most *VilCre;Catnb*$^{flox/flox}$ animals die during embryonic development, with rare survivors showing a mosaic pattern of β-catenin inactivation in the colon. Black arrows indicate *β-catenin*-deficient crypts and red arrows indicate normal crypts in a mosaic colon. An antibody that detects both YAP and TAZ was used in the analysis (see Experimental Procedures for details).

(F) β-catenin and YAP/TAZ staining in control and *Yap/Taz* double mutant (*VilCre;Yap*$^{flox/flox}$*;Taz*$^{flox/flox}$) distal colon at 1-month of age. Note the similar β-catenin staining in control crypts (red arrow, positive staining for YAP/TAZ) and *Yap/Taz* double mutant crypts (black arrow, negative staining for YAP/TAZ).

Figure S4

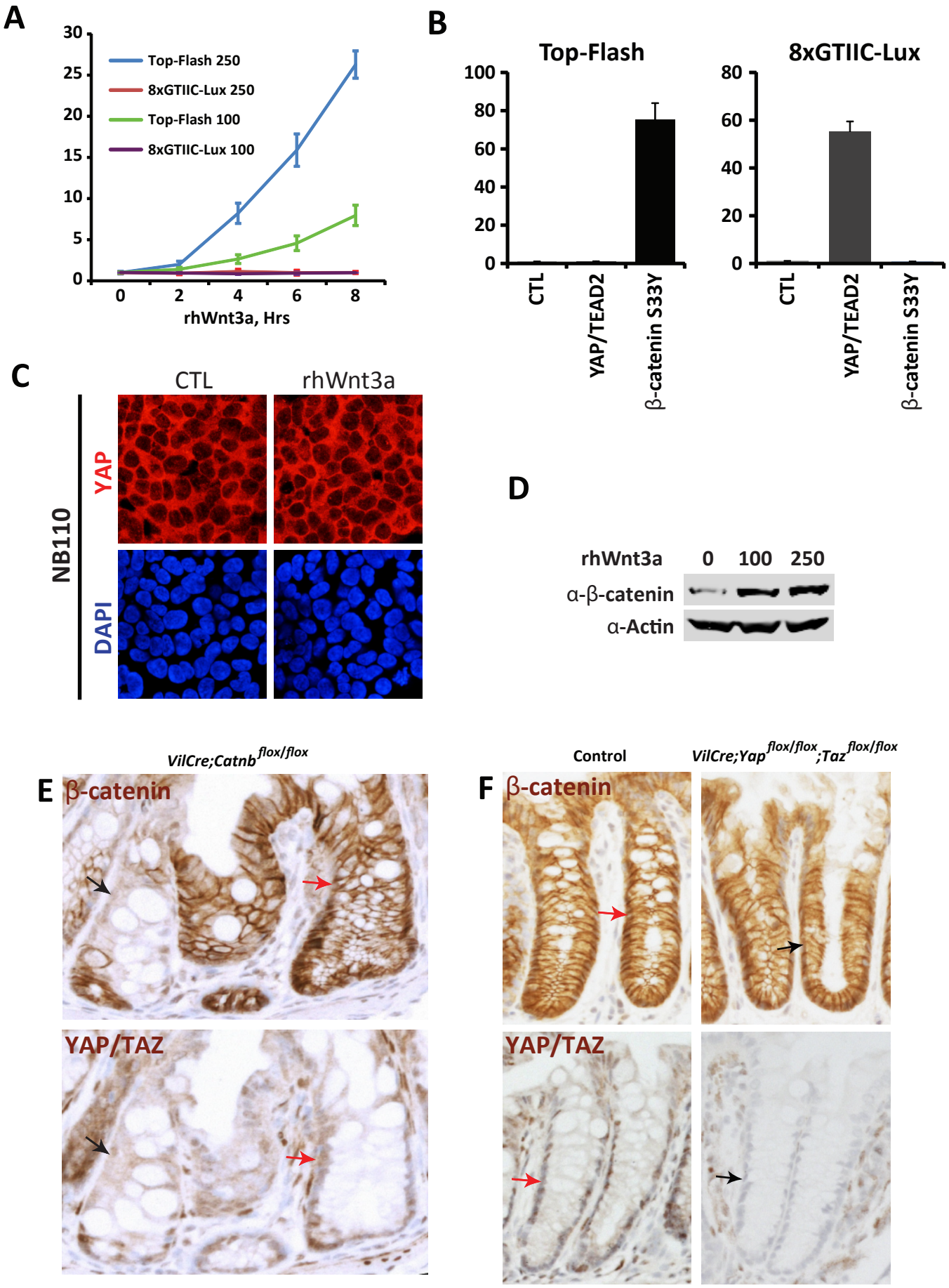
A
30
25
20
15
10
5
0
0
2
4
6
8
rhWnt3a, Hrs
Top-Flash 250
8xGTIIC-Lux 250
Top-Flash 100
8xGTIIC-Lux 100
B
Top-Flash
8xGTIIC-Lux
100
80
60
40
20
0
CTL
YAP/TEAD2
β-catenin S33Y
C
CTL
rhWnt3a
NB110
YAP
DAPI
D
rhWnt3a
0
100
250
α-β-catenin
α-Actin
E
VilCre;Catnb flox/flox
β-catenin
YAP/TAZ
F
Control
VilCre;Yap flox/flox;Taz flox/flox
β-catenin
YAP/TAZ

Figure S5. Validation of YAP antibodies: not all commercial YAP antibodies are specific.
(A) Lysate from HEK293 cells after siRNA knockdown of YAP was probed with different YAP antibodies. **H-9**: Santa Cruz Biotechnology, sc-271134; **4912**: Cell Signaling Technology, #4912; **NB110**: Novus Biologicals, NB110-58358; **63.7**: Santa Cruz Biotechnology, sc-101199. While 4912, NB110 and 63.7 recognized a ~65 KDa signal that was abolished by YAP RNAi (arrowheads), H-9 did not recognize a specific signal that was abolished by YAP RNAi, suggesting that H-9 is not specific to YAP.
(B-C) The H-9 YAP antibody revealed cytoplasmic staining in both sparse and dense HEK293 cultures (B), and the signal remained after YAP RNAi (C), suggesting this antibody is not specific to YAP.
(D-E) The NB110 antibody revealed nuclear staining when HEK293 cells were sparse and cytoplasmic staining when cells were dense (D), and the signal was dramatically decreased after YAP RNAi (E), suggesting that this antibody is specific to YAP.

Figure S5

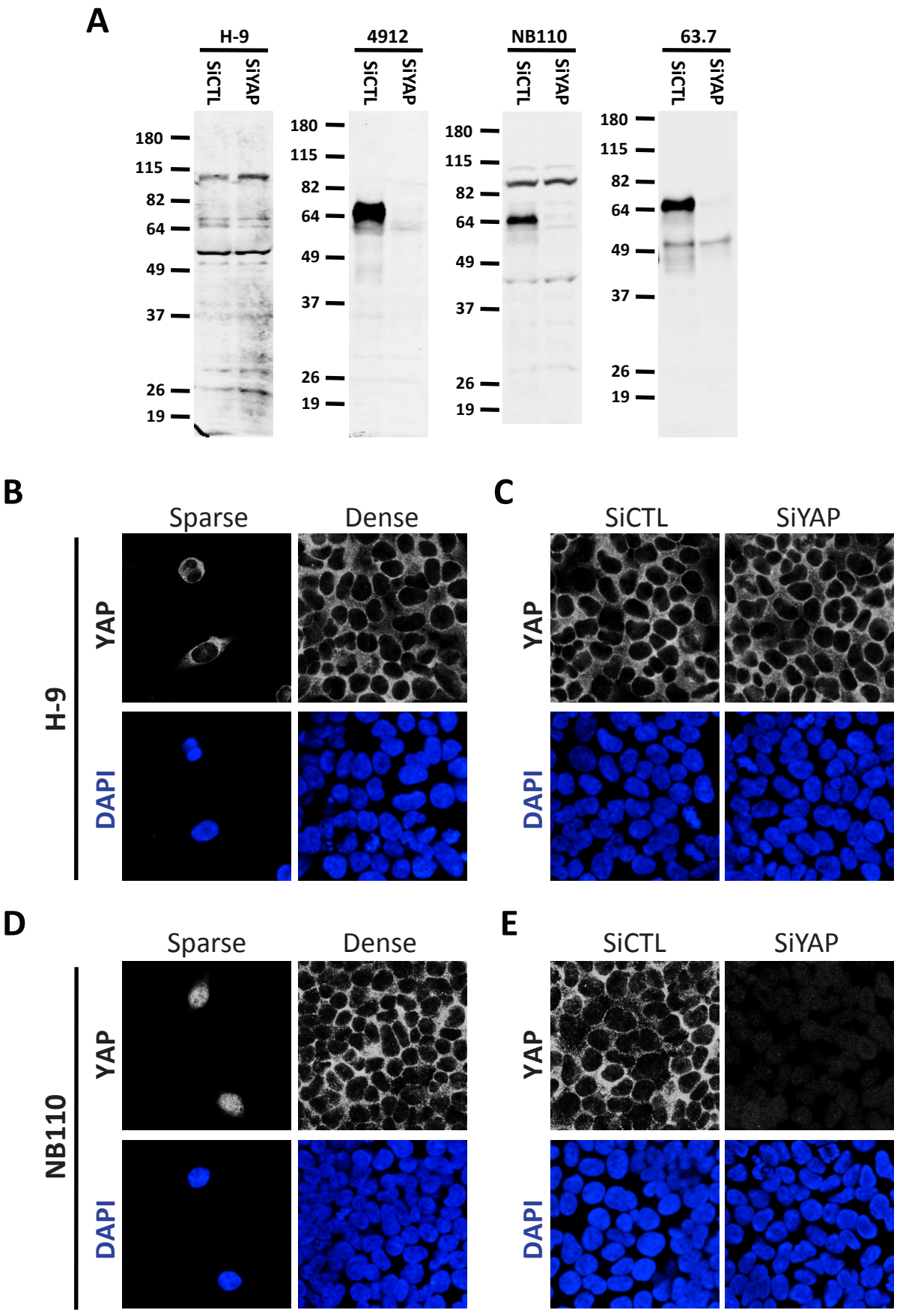
A
H-9
4912
NB110
63.7
SiCTL
SiYAP
180
115
82
64
49
37
26
19
B
Sparse
Dense
H-9
YAP
DAPI
C
SiCTL
SiYAP
YAP
DAPI
D
Sparse
Dense
NB110
YAP
DAPI
E
SiCTL
SiYAP
YAP
DAPI

Figure S6. Tumorigenesis in *β-catenin*$^{\Delta ex3}$ mutant, *β-catenin*$^{\Delta ex3}$*;Sav1* double mutant and *APC* mutant jejunum.

Histological analysis of *β-catenin*$^{\Delta ex3}$ (*Lgr5-EGFP-IRES-creER*^{T2}*;Catnb*$^{+/lox(ex3)}$), *β-catenin*$^{\Delta ex3}$*;Sav1* double mutant (*Lgr5-EGFP-IRES-creER*^{T2}*;Catnb*$^{+/lox(ex3)}$*;Sav1*$^{flox/flox}$) and *APC* mutant (*Lgr5-EGFP-IRES-creER*^{T2}*;APC*$^{flox/flox}$) jejunum 4 weeks after tamoxifen injection. Note the larger polyps in *β-catenin*$^{\Delta ex3}$*;Sav1* double mutant and *APC* mutant jejunum compared to *β-catenin*$^{\Delta ex3}$ jejunum. Black arrows indicate adenomatous transformation. Scale bar, 100 μm.

Figure S6

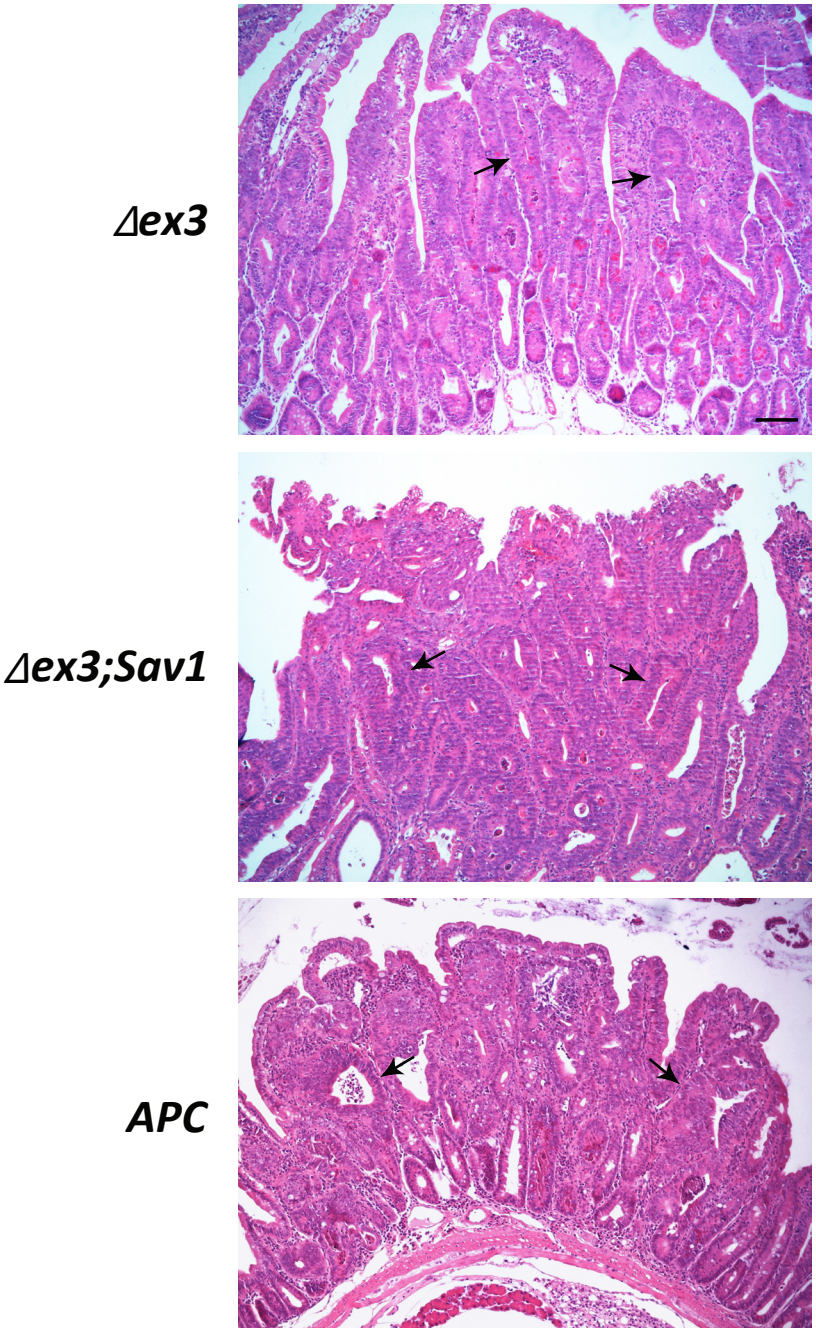

Figure S7. Loss of YAP suppresses intestinal tumorigenesis in *VilCre;APC^{flox}*/+ mice.

(A) Quantification of the number of adenomas in the small intestine and the colon of 16 *VilCre;APC^{flox}*/+ (*APCHet*) and 23 *VilCre;APC^{flox}*/+*;Yap$^{flox/flox}$* (*APCHet;Yap*) mice at the age of 4.5-month. Note the completely abolished tumor formation in *APCHet;Yap* small intestines after inactivation of YAP. (*) $P<0.001$, (n.s.) not significant, *t*-test.

(B-C) Analysis of the neoplastic jejunal epithelia in 4.5-month-old *APCHet;Yap* mice. (B) H&E staining. Black arrow indicates neoplastic colonic epithelia and red arrow indicates their non-neoplastic neighbors. (C) YAP staining. Note the absence of YAP staining in the non-neoplastic epithelia (red arrows) and positive YAP staining in their neoplastic neighbors (black arrows). Scale bar, 100 μm.

Figure S7

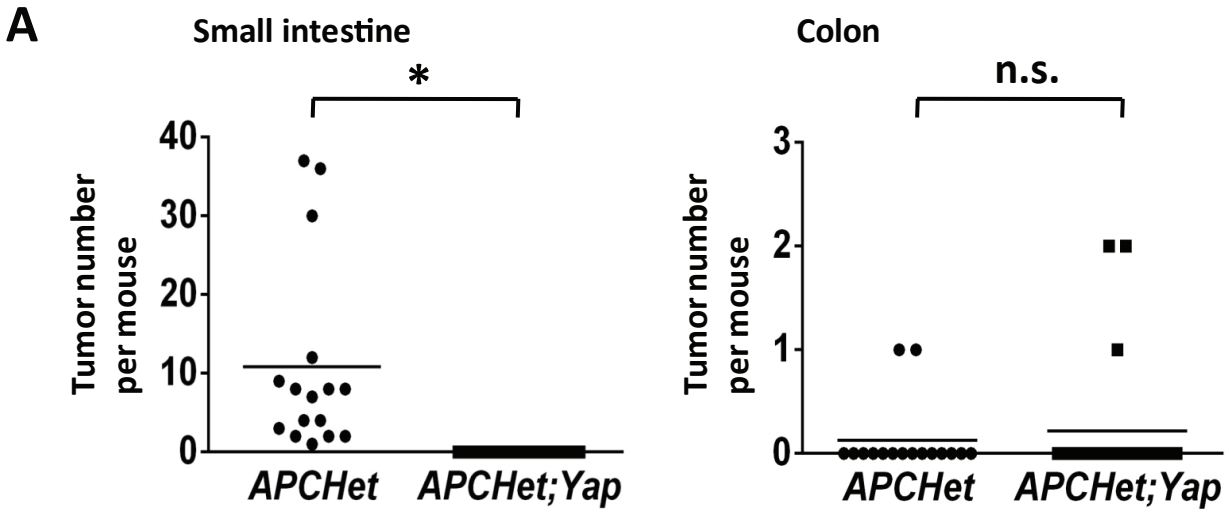

VilCre;APC$^{flox/+}$;Yap$^{flox/flox}$